Determination of the sticking coefficient and scattering dynamics of water on ice using molecular beam techniques

K. D. Gibson, Daniel R. Killelea, Hanqiu Yuan, James S. Becker, and S. J. Sibener[a)]

The James Franck Institute and Department of Chemistry, The University of Chicago, 929 E. 57th Street, Chicago, Illinois 60637, USA

The sticking coefficient for D_2O impinging on crystalline D_2O ice was determined for incident translational energies between 0.3 and 0.7 eV and for H_2O on crystalline H_2O ice at 0.3 eV. These experiments were done using directed molecular beams, allowing for precise control of the incident angle and energy. Experiments were also performed to measure the intensity and energy of the scattered molecules as a function of scattering angle. These results show that the sticking coefficient was near unity, slightly increasing with decreasing incident energy. However, even at the lowest incident energy, some D_2O did not stick and was scattered from the ice surface. We observe under these conditions that the sticking probability asymptotically approaches but does not reach unity for water sticking on water ice. We also present evidence that the scattered fraction is consistent with a binary collision; the molecules are scattered promptly. These results are especially relevant for condensation processes occurring under nonequilibrium conditions, such as those found in astrophysical systems. © *2011 American Institute of Physics*. [doi:10.1063/1.3528116]

I. INTRODUCTION

The sticking of gas-phase molecules onto surfaces is the initial step in many important processes. For instance, the first step in reactions proceeding through a Langmuir-Hinshelwood mechanism is the adsorption of the reactants to the surface.[1] Another example is ozone depletion due to reactions with Cl containing species in polar stratospheric clouds (PSC).[2] The type II PSCs consist mainly of water ice.[3] HCl is one reactive species that can be adsorbed by type II PSCs, but it does not dissociate on the ice surface[4] and must be incorporated into the crystal either during the collision[5] or by adsorption of more water molecules. If the reactions take place inside the ice crystals, then the rates at which water molecules evaporate and condense from the surface affect the lifetimes of absorbed species and whether they undergo reaction.[6,7]

In addition to atmospheric phenomenon, the sticking of water on ice is important for understanding the behavior and development of icy bodies in space. Subtle changes in sticking may have profound effects over astronomical time scales in the aggregation of icy mantles on small particles.[8–11]

In our experiments, the sticking coefficients (S) of D_2O and H_2O on crystalline ice (CI) were determined using molecular beam techniques. Molecular beams allow precise control of both the incident energy and angle, allowing for a detailed understanding of the sticking process.[12] Water sticking to ice is a highly probable process due to efficient energy accommodation of the incident molecules. Excess incident translational energy (E_I) is readily absorbed by the ice from efficient momentum transfer to the lattice because of the identical mass of the projectile and the target. Two previous beam experiments are particularly relevant to the results presented here. Brown

et al.[13] found the H_2O sticking coefficient on H_2O ice to be 0.99 ± 0.03 for incident angles $\Theta_I = 0°$ –$70°$ and incident beam energies $E_I = 0.04$–1.7 eV. Batista *et al.*[14] also used H_2O, with incident energies of 0.5–1.5 eV. They found that S was essentially one at lower incident energies but significantly decreased when the velocity component of the incident water molecules parallel to the ice surface ($v_{\parallel}$) was large, $\approx 10^3$ m/s or greater. Their model interprets the $v_{\parallel}$ dependence as due to the strong corrugation of the water molecule-ice potential with both the lateral position in relation to the surface and the orientation of the incoming molecule being of importance.

The experiments presented here examined in detail the sticking for D_2O molecules with incident energies between 0.3 and 0.7 eV. In addition to determining the sticking coefficients, our experiments measured the intensity and final energy (E_F) of D_2O molecules scattered off a crystalline D_2O ice surface as a function of exit angle (Θ_F). These high precision measurements allow for a more complete understanding of the dynamics of water sticking. The results expand upon the Batista *et al.* study, with greater precision in the very high sticking regime and to lower incident energies, as well as our direct measurements of the scattering dynamics for the nonsticking molecules. Moreover, in complementary experiments, Fourier-transform reflection-absorption infrared spectroscopy (IRRAS) was used to measure the uptake of D_2O and H_2O on their respective crystalline ice surfaces at several surface temperatures.

II. EXPERIMENTAL DETAILS

The scattering experiments were performed in an ultrahigh vacuum (UHV) chamber (base pressure 10^{-10} Torr) with the capability of having up to three independent molecular or atomic beams impinging simultaneously on a

---

a)Author to whom correspondence should be addressed. Electronic mail: s-sibener@uchicago.edu.
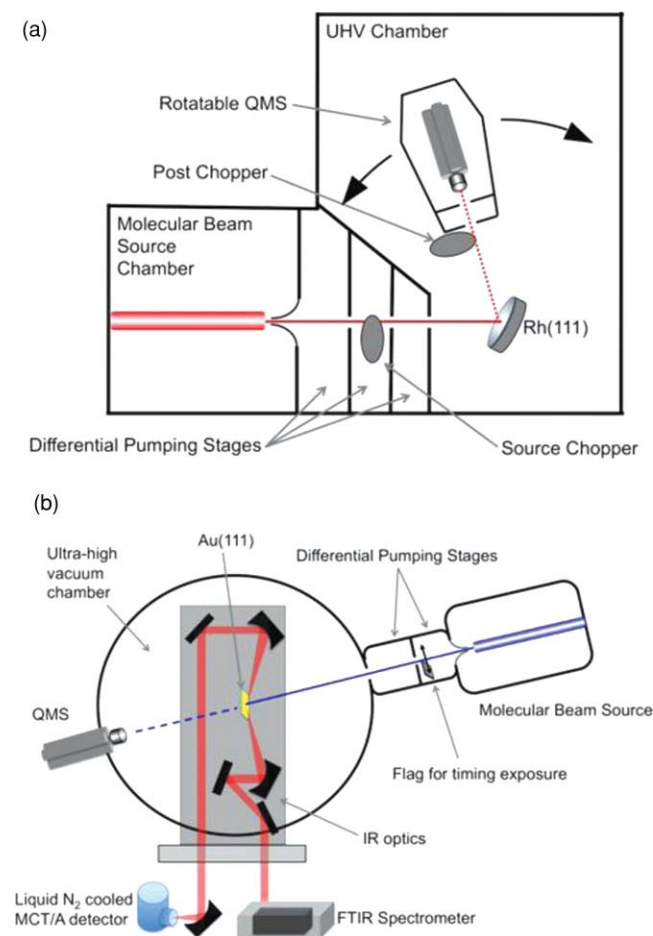
(a)

(b)

FIG. 1. Schematics of experimental apparatus. (a) UHV scattering chamber with a differentially pumped, rotatable QMS. (b) UHV scattering chamber with a single molecular beam and IRRAS detection.

target crystal. A schematic is shown in Fig. 1. A Rh(111) single crystal was mounted on a manipulator that allows for the adjustment of the incident polar angle (Θ_I), was cooled with liquid N_2, and resistively heated. A double-differentially pumped quadrupole mass spectrometer (QMS) was used for detecting the scattered molecules. The detector can be rotated with respect to the target crystal so that the scattering angle investigated can be varied independently from the incident angle. The same detector was also used for temperature-programmed desorption (TPD), where the surface temperature (T_S) is ramped while collecting the signal from desorbing molecules. The IRRAS experiments, schematically shown in Fig. 1, were conducted in a separate UHV chamber with a single molecular beam source.[15] The Au(111) single crystal was mounted on a five-axis manipulator and could be cooled below 120 K with liquid N_2 and radiatively heated above 1000 K to clean the Au(111) substrate. IR spectra were taken at a resolution of 4 cm^{-1} and averaged over 100 scans. The O-D or O-H stretch regions were integrated to quantify the D_2O or H_2O coverage.

The water beams used in the scattering experiments were made by bubbling He or H_2 through a heated reservoir (345 K) of D_2O. The heated reservoir increased the partial pressure of D_2O significantly, allowing for a more intense

beam. To prevent condensation in the tubing leading to the nozzle, the lowest nozzle temperature was 373 K, thus establishing the minimum incident energy we could achieve. D_2O was used because the m/e = 20 background in the differentially pumped mass spectrometer detector was less than that for m/e = 18. The expansion was through a heatable nozzle (373–673 K) with a 50 μm pinhole at a backing pressure of ~40 psi. Various E_I could be achieved by seeding the D_2O in different carrier gases (H_2 or He) and adjusting the nozzle temperature. At the incident angles used in these experiments, the entire beam was intercepted by the target. It is worth noting that when using H_2 as the carrier gas at elevated nozzle temperatures, there was significant H–D exchange between D_2O and H_2. This resulted in the H_2 seeded beams containing a significant amount of HDO. However, we were able to avoid this problem by seeding D_2O in He. By heating the nozzle, we could make beams that were nearly as fast as those seeded in H_2. Within the precision of our measurements, there was no carrier gas dependence in the D_2O scattering. For the IRRAS data, only a single incident energy was used at normal incidence. Helium was bubbled through either D_2O or H_2O in a room-temperature bubbler and expanded through a heatable nozzle with 150 μm orifice with a backing pressure of 20 psi, yielding a beam with an average E_I of 0.3 eV.

For the scattering experiments, one differentially pumped region of the molecular beam source contained a shutter, which could block the beam for precise timing of exposure duration, and a mechanically rotated chopper for modulating it. This chopper had two sets of slots. Narrow slots could be used for measuring the incident energy distributions by time-of-flight (TOF) measurements. This was done by lowering the target out of the beam path and rotating the detector to look directly at the beam. Examples of the derived energy distribution of the incident beams are shown in Fig. 2. As shown, the energy distributions are symmetric and narrow, thus the average energy is an appropriate value for the ensemble. There were also two larger slots, each with a 25% duty cycle, for looking at a square-wave modulated signal. There was also a cross-correlation chopper attached to the detector that could be used to measure the E_F of the scattered D_2O.

For the scattering experiments, the target substrate was a Rh(111) crystal. It was cleaned by Ar$^+$ sputtering at 900 K, followed by exposure to O_2 at 900 K and annealing to
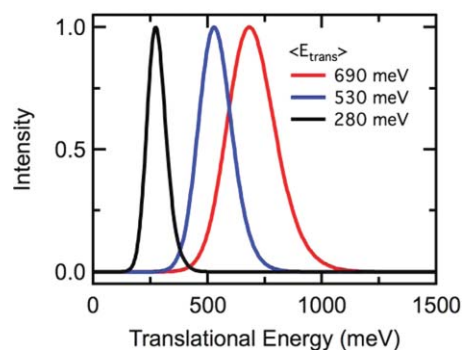

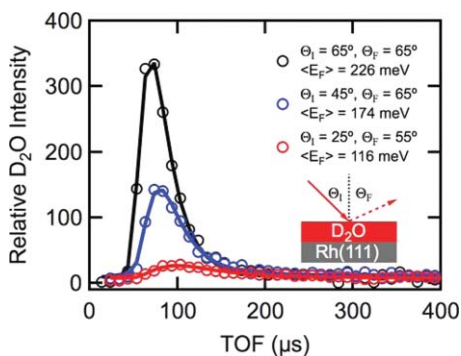FIG. 2. Incident energy distributions for three different D_2O beams.

FIG. 3. TOF spectra of scattered D_2O. The spectra were taken at three different Θ_I, $\langle E_I \rangle$ = 690 meV, and T_S = 140 K. Spectra were taken using the chopper attached to the detector and the points are the deconvoluted results. The solid lines are fits to the data (see text).

FIG. 4. Examples of square-wave spectra. The intensity of scattered D_2O was measured for two different $\langle E_I \rangle$ with T_S = 140 K, Θ_I = 45°, and Θ_F = 65°.

~1250 K. Once the crystal was initially cleaned enough to deplete the impurities from the selvedge, just exposing it to oxygen and then annealing for a few minutes was sufficient to remove adsorbed impurities. The clean Rh(111) was cooled to 450 K and exposed to a room temperature O_2 beam so as to grow an ordered half-monolayer of adsorbed atomic oxygen.[16] The crystal was then cooled to the surface temperature of the scattering experiment and exposed to a room temperature beam of D_2O entrained in He for a sufficient time to grow an ~100 layer ice overlayer. The coverage was measured by integrating TPD spectra and calibrated with the signal of a desorbing D_2O monolayer grown on the clean Rh(111) crystal.[17]

This procedure led to an ice layer that showed no long-range order with surface-sensitive He scattering, which showed at best a small specular peak and no other diffraction peaks. At T_S = 140 K, the temperature of most of these experiments, the surface was completely covered with D_2O as determined by $CHCl_3$ adsorption and TPD.[18,19] The sticking coefficient in the scattering experiments was always nearly one, so that while the measurements were made a few thousand layers could build up on the surface.

The Au(111) sample for the IRRAS data was cleaned with Ar^+ sputtering at 773 K followed by annealing at 973 K for 30 min.[20] Cleanliness was verified using Auger electron spectroscopy and (111) surface order was checked using low-energy electron diffraction. Once the Au(111) sample was cooled to ≈120 K, IRRAS measurements showed almost no background absorption (i.e., H_2O, CO_2) over a period of hours.

We did three types of scattering experiments. The first gave the most extensive information and involved using the detector-mounted chopper to measure both the energy and intensity of the scattered water as a function of Θ_I and Θ_F. Examples of the TOF spectra are shown in Fig. 3. When the scattered signal was too small to make these doubly differential measurements, square-wave chopping was used to get the total intensity as a function of angle; examples are shown in Fig. 4. Both types of experiments measured in-plane scattering. This plane contained both the incident beam and the arc defined by the detector motion, with the ice surface perpendicular to this plane. These measurements gave relative scat-
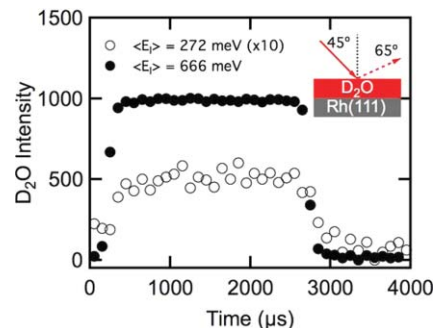
tering probabilities, assuming that the ice surface that grew was the same at all incident velocities.[21]

However, a different measurement was needed to determine the absolute amount scattered. This was accomplished by slowly modulating the incident beam with the shutter in the differentially pumped beam source region and monitoring the total scattered D_2O signal with a residual gas analyzer that was not in a direct line-of-sight with the target. This signal was due to molecules that had scattered from the surface and then undergone further collisions with the walls of the vacuum chamber. Therefore, these molecules are thermalized with the walls at 300 K and integrated over all of the final scattering angles. By comparing measurements at both T_S = 250 K, where there is no sticking, and the temperature where the other measurements were made, an absolute measure of the scattering (or sticking) fraction could be determined. An example is shown in Fig. 5.

Quantification of the IRRAS data was not as straightforward as the TPD data discussed above. Water does not wet the Au(111) surface, and there is no unique metal–water layer to quantify surface coverage. To determine our coverage, we first measured the incident flux of D_2O and H_2O directly using a liquid N_2 cooled Au-coated, 1.3 cm diameter quartz–crystal microbalance (QCM). When the QCM was exposed to the molecular beam, no increase in the water background was seen with the QMS in the UHV chamber, indicating the sticking was near unity on the QCM. The QCM measured
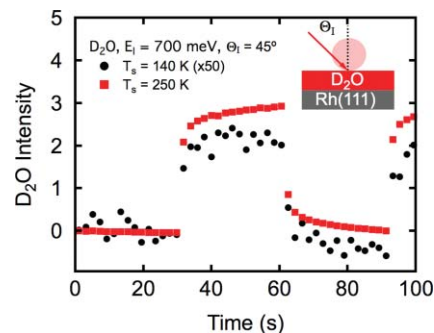

FIG. 5. Determination of absolute scattering fraction. An example of the results for the slow-modulation experiments. The D_2O scattered from a warm surface (red squares) was compared to the scattering from a cold surface (black circles). The results for T_S = 140 K have been multiplied by 50 for clarity.
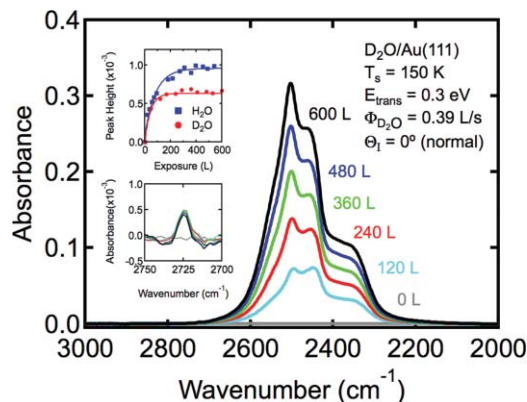
FIG. 6. IRRAS spectra of D_2O on Au(111) at various exposures. The lower inset plot is the dangling O–D region of the spectrum for each trace in the main panel. The upper inset plots the dangling O–D or O–H peak height vs exposure for D_2O and H_2O and shows the peak saturating for both isotopologues by 150 L exposure.

an uptake of $(2.9 \pm 0.5) \times 10^{-9}$ g cm^{-2} s^{-1} for D_2O and $(2.0 \pm 0.4) \times 10^{-9}$ g cm^{-2} s^{-1} for H_2O. The beam impinged on a circular spot of 6 mm and defining 1 L (layer) to be 1.06×10^{15} molecules cm^{-2},[13] the incident flux (Φ) was, therefore, determined to be 0.39 ± 0.07 L D_2O s^{-1} and 0.30 ± 0.06 L H_2O s^{-1}. In summary, use of the deposition procedures and ice thicknesses discussed above in the scattering measurements that used a Rh(111) support substrate and in the complementary IRRAS measurements that used a Au(111) support substrate produced ice surfaces for this study that were indistinguishable from each other.

The IRRAS data (Fig. 6) clearly show the film was crystalline,[21] and the absorption features in the O–D stretch region increased linearly with coverage above $\approx$120 L exposure. The small IRRAS peak at 2725 cm^{-1} (Fig. 6, lower inset) corresponds to undercoordinated, dangling O–D bonds (3700 cm^{-1} for H_2O) at the ice–vacuum interface.[22] The intensity of this peak was related to the surface area of the ice film, and it saturated (Fig. 6, upper inset) at about 100 L D_2O exposure, indicating the area of the vacuum–surface interface was constant with higher coverage. Results from H_2O were analogous but reached the homogeneous region at a slightly greater coverage, as shown in the upper inset of Fig. 6.

The desorption rate of water from the ice surface was quantified at several temperatures between 140 and 165 K using IRRAS in order to relate the measured IR peak intensities to coverage (L) of D_2O or H_2O and to correct for the water that desorbed during the dose at the higher surface temperatures in this study. Although the metal substrate plays a key role in the morphology of deposited ice films, water on Au(111) behaves the same as other substrates above $\approx$150 L coverage.[23] The observed desorption was the same as that from bulk ice; once the $\approx$120 L threshold was reached, the integrated absorption intensity was linear for both desorption and uptake and no new features emerged in the IR spectra (Fig. 6). From the IRRAS data, the activation energy for D_2O desorption from crystalline D_2O was calculated to be 0.51 ± 0.02 eV with a prefactor of 1.3×10^{14} Abs s^{-1} and for H_2O, $E_a = 0.50 \pm 0.02$ eV and $A = 2.4 \times 10^{14}$ Abs s^{-1}. These values are in good agreement with Speedy *et al.*,[24] and
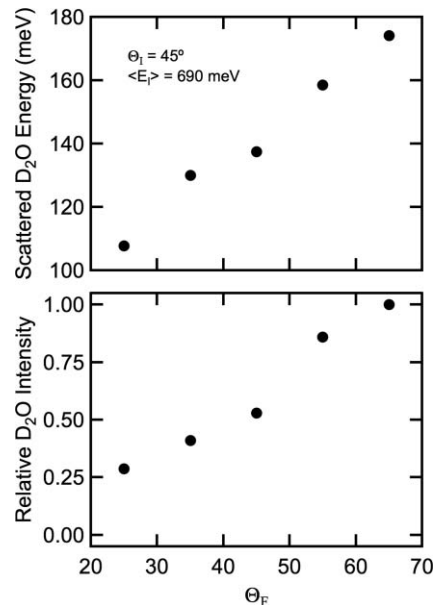

FIG. 7. Angular dependence of the energy and intensity of D_2O scattered from a crystalline ice surface at $T_S = 140$ K. Data are calculated from TOF measurements similar to those shown in Fig. 3.

thus we use the desorption rates to connect our integrated absorbance (Abs) to ice coverage (L). Finally, the sticking coefficient was calculated using Eq. (1), where θ_{IRRAS} is the water coverage measured with IRRAS, θ_{des} is the amount of water that desorbed during the dose, Φ is the incident flux of either D_2O or H_2O, and t is the dose time. S was always found to be linear at coverages greater than 120 L of water.

$$ S = \frac{\theta_{IRRAS} + \theta_{des}}{\Phi t}. \tag{1} $$

III. RESULTS AND DISCUSSION

Figure 3 shows illustrative deconvoluted TOF spectra (points) and fits to the data (lines). For all of the TOF spectra, a single shifted Maxwell–Boltzmann velocity distribution, given by Eq. (2), describes the data well,

$$ f(v) \propto v^3 \exp(-[(v - v_0)/a]^2). \tag{2} $$

Surface scattering often shows two components; the first is fast molecules impulsively (directly) scattering from the surface. The second are slower molecules which first thermalized with the surface and then desorbed, the trapping-desorption (TD) channel.[25] At the surface temperature of these experiments, $\leq$140 K, no TD feature was observed; once water trapped on the surface it did not desorb, consistent with the zeroth-order desorption parameters of Speedy *et al.*,[24] $A = 1 \times 10^{16}$ L s^{-1} and $E_a = 0.5256$ eV. Figures 7 and 8 show examples of how the final energy and intensity vary with Θ_F. The general features are consistent with all of the scattering data taken; both the final energies and intensities increase at more glancing final angles. The top panel of Fig. 9 shows how the ratio of final to initial energy varies. It shows that, at least for the higher incident energies, the percentage of energy exchanged with the surface was not dependent on the
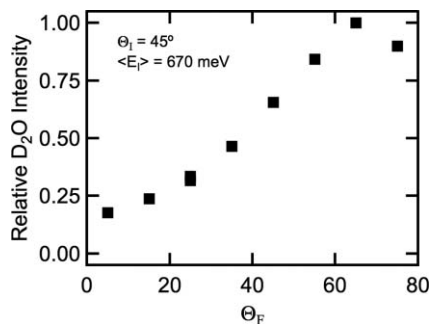
FIG. 8. Angular dependence of the intensity of D_2O scattered from a crystalline ice surface at $T_S = 140$ K. Data are calculated from square-wave chopping measurements similar to those shown in Fig. 4.

initial energy. Although sputtering of D_2O from the ice surface by the incident beam was possible, there is no reason to expect that any of the D_2O leaving the surface was the result of sputtering. Water sputtering has been shown to be improbable even at very high (10–20 eV) incident energies.[26] Furthermore, the incident energy of the beam (0.3–0.7 eV) was not much more than the activation energy for desorption, $E_a = 0.53$ eV,[24] which is a good approximation of the surface binding energy. Thus, after the initial collision there would be little, if any, energy left for the desorbing D_2O molecules, even in the absence of rapid quenching by the ice lattice.

These two observations, that the final energy and intensity are greatest for larger included angles ($\Theta_I + \Theta_F$) and that the percentage of energy exchange with the surface is independent of the incident energy, are both consistent with the water having undergone a simple binary collision.[27] A good comparison would be with the D_2O scattering from glycerol,[28] where there was also a strong hydrogen-bonding
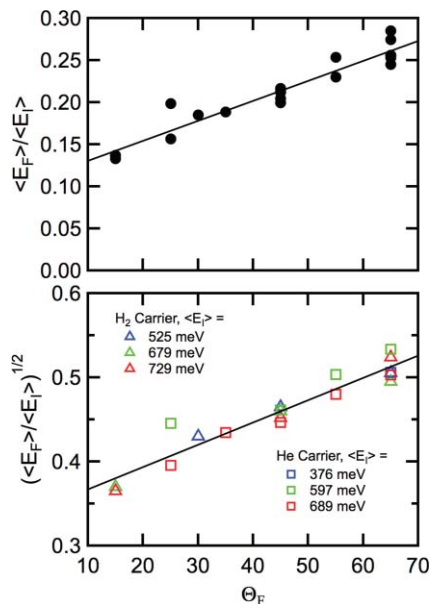

FIG. 9. Fractional energy loss of D_2O scattered from the crystalline ice surface as a function of Θ_F (top). The bottom panel shows the data plotted as the square root of the energy ratio for D_2O seeded in both H_2 and He and three different incident energies. All data were collected for $\Theta_I = 45^o$ and $T_S = 140$ K.
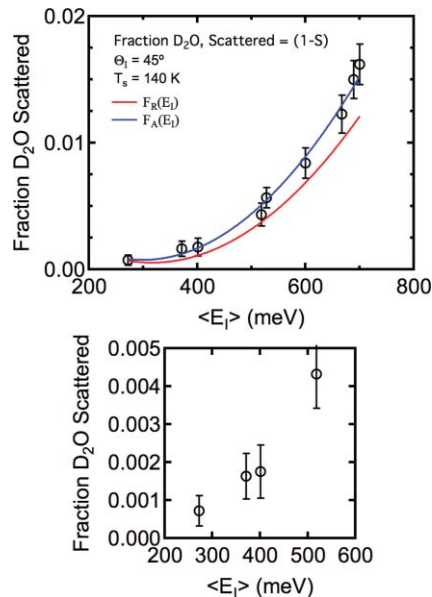

FIG. 10. Fraction of D_2O scattered from crystalline ice at $T_S = 140$ K and $\Theta_I = 45°$. The fraction of D_2O scattered from the ice surface $(1-S)$ is shown for incident energies from 200 to 800 meV. For an explanation of the lines, see text. The lower panel highlights the high sticking portion below 600 meV. Even at the lowest incident energies, scattering was observed, indicating that $1-S$ does not reach zero under any of the conditions examined herein.

interaction. Molecular dynamics simulations for this system[29] show that molecules in the impulsively scattered (IS) channel (the only scattering channel we see) were qualitatively described by a simple kinematic encounter; the repulsive part of the potential was most important during the initial interaction.[29] The intensity of the scattering does depend on the surface structure, the collision was most likely with only a few surface molecules and will partially depend on parameters such as the surface roughness.

As mentioned in Sec. II, the initially prepared ice surface exhibited no long-range order when analyzed using surface-sensitive He scattering. The ice grown at 140 K was crystalline; there was only one peak in the D_2O TPD spectra where amorphous solid water (ASW) would have shown two desorption peaks; additionally, the IRRAS data showed the ice to be crystalline as well.[21,24] Because of these factors, the surface was essentially polycrystalline ice with no azimuthal ordering. The D_2O TPD spectra were the same for all studied incident energies, indicating that the ices all had the same structure, consistent with the results of Smith *et al.*[13,21] The exact nature of the surface, i.e., its roughness at the atomic level, could not be determined in these studies. However, the surface here was a good model for naturally occurring ice crystals that form on condensation nuclei, such as dust grains in the interstellar medium.

It was also possible to map out the scattering (or sticking) probability using all of the data from the different types of experiments. The results for $\Theta_I = 45°$ are shown in Fig. 10. Using a slow modulation experiment, the sticking coefficient at an average incident energy of 700 meV was found, quite precisely, to be 0.985 ± 0.003. This anchors the absolute value at the right side of the plot. To determine S from TOF data, it was then only necessary to normal-

ize by the incident intensity and then multiply by a factor that aligns the high-energy results with a scattering fraction, $F(E_I) = (1 - S)$ of 0.015. For the square-wave modulated experiments, one further correction was necessary. Because the detector uses electron bombardment ionization, the measurements gave the number density of the D_2O. To convert this to flux, the velocity of the D_2O was needed. This was estimated by using a fit to $(\langle E_F \rangle / \langle E_I \rangle)^{1/2}$ versus Θ_F as shown in the bottom panel of Fig. 9. The points in Fig. 10 represent the fraction of water molecules scattered from the ice surface as a function of incident translational energy, E_I, plotted against the average energy of the energy probability distributions. These data are the *apparent* scattering fraction, $F_A(E_I)$ for an ensemble of D_2O molecules with a distribution of translational energies, $P(E_I)$ as shown in Fig. 2. To determine $F_R(E_I)$, the *real* scattering fraction as a function of E_I, a quadratic least-squares fit to the data (blue line, Fig. 10) was used to quantify $F_A(E_I)$, the apparent fraction of scattered D_2O. $F_A(E_I)$ is an overestimation of the *real* fraction scattered because of the widths of the energy distributions of the incident D_2O molecules are nonzero. In order to extract the real scattering fraction from the data, this fit was used as shown in Eq. (3) and $F_R(E_I)$ is represented by the red line in Fig. 10.

$$F_A(E_I) = \int F_R(E_I)P(E_I)dE_I. \tag{3}$$

Though $F_R(E_I)$ becomes quite small it never goes to zero, even at the lowest incident energy, thus *S never reaches unity*.

The nozzle was heated to elevated temperatures (373–673 K) to increase E_I and vibrational excitations of the D_2O molecules may affect the observed sticking. However, under the conditions employed in this study, it is unlikely that internal excitations are a factor. First, a harmonic oscillator model predicts that less than 3% of D_2O molecules are vibrationally excited at the highest nozzle temperature used. Second, internal excitations have not been observed to affect physisorption for both thermal ensembles[30] and in state-resolved studies.[31] Third, in the data presented here there was no observable difference in the scattering for beams with nearly the same E_I but different nozzle temperatures. For instance, the points at 370 and 400 meV were taken with nozzle temperatures of 473 and 373 K, respectively, and the points at 520 and 530 meV were taken with nozzle temperatures of 663 and 473 K, respectively, but the data are indistinguishable within the precision of the measurements.

For $E_I \sim 0.7$ eV, some experiments were done at different Θ_I. Examples of the TOF spectra are shown in Fig. 3. These show the general trend that the final intensity and energy peak at glancing Θ_F. The absolute measure of S was found to be 0.990, 0.985, and 0.980 at $\Theta_I = 25°$, $45°$, and $65°$, respectively, all accurate to ± 0.003.

The sticking coefficients for D_2O and H_2O on their respective ices were measured with IRRAS at surface temperatures between 140 and 155 K and were found to be 0.98 ± 0.03 for both isotopologues; much more precise data on S were obtained by detecting the reflected molecules, measurements which intrinsically indicate nonunity sticking. Within the experimental error, no trend in S was found with respect to the surface temperature and S was found to be vir-
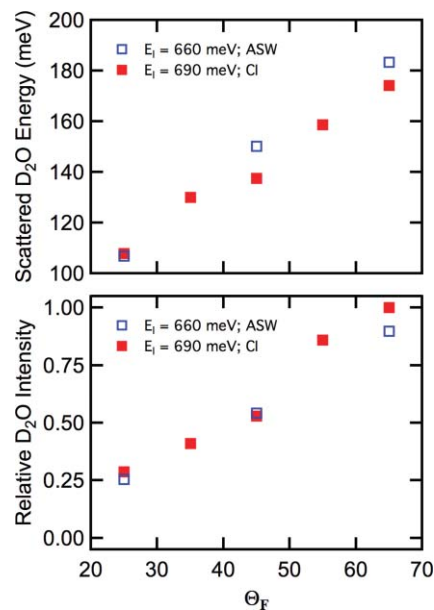

FIG. 11. D_2O scattering from ASW and CI. The angular dependence of the energy and intensity of D_2O scattered from ASW at 110 K and CI at 140 K and $\Theta_I = 45°$ are shown. The two datasets are indistinguishable within the experimental limits.

tually the same for both D_2O and H_2O on their respective ices. The uncertainty associated with the IRRAS measurements was found to be significantly higher under conditions with near unity sticking than for corresponding measurements where the scattered fraction was measured. This was the result of attempting to measure very small changes in the large IR absorption feature of the ice film.

Finally, a few experiments were performed to investigate the scattering dynamics from a metastable, noncrystalline phase of water, ASW. Here, the initial D_2O deposition and subsequent measurements were performed at $T_S = 110$ K. The scattering data from ASW are compared with CI ($T_S = 140$ K) in Fig. 11. At 110 K, the rate of conversion from ASW to CI is extremely slow,[19] so the ice remained amorphous throughout the measurements. This was confirmed by the presence of two desorption features in the TPD spectrum. There were no appreciable differences in the intensity or energy of D_2O scattered from ASW or CI.

IV. CONCLUSIONS

The sticking of D_2O onto D_2O ice at incident energies between 0.3 and 0.7 eV has been examined in detail. These experiments were done with directed molecular beams, allowing for precise control of the incident angle and collisional energy. These experiments also measured the intensities and energies of the scattered fractions as a function of scattering angles, giving new insights into the dynamics of water sticking on ice surfaces. These scattered fractions were consistent with a binary collision model; the molecules were scattered promptly. These sticking data agree quantitatively and significantly expand upon those of Batista *et al.*,[14] and complement them by providing precise measurements of S in a regime where it approaches, but does not reach, unity, and furthers our understanding of the water–ice interaction by measuring

the collision dynamics for the nonsticking (directly reflected) molecular fraction.

Comparing the results from the scattering experiments to the IRRAS data highlights the power of combining the information derived from these two methods. The highly precise measurements of the scattered fraction to determine S are perfectly suited for conditions where sticking is near unity, where IRRAS measurements have difficulty discerning small changes in S. However, these scattering measurements allow us to pin the value of S. As S deviates from unity, the integrative nature of the IRRAS (or QCM) measurements allow for full mapping of the sticking coefficient function across a wide-range of S values.

These results show that the sticking of water on ice is never unity in the range of incident energies and angles examined. Even at the lowest incident energy, some D_2O was scattered, with precise scattering measurements indicating that $1-S$ never goes to zero, even under the lowest energy (most gentle) conditions examined herein. The sticking probability was near unity for all measurements presented in this study. Although the scattered fraction increases slightly with increasing incident energy, the morphology and temperature of the ice surface have little effect on the sticking probability. These results are of fundamental interest to the interfacial dynamics of nonequilibrium processes, including astrophysical processes, given that the sticking probability asymptotically approaches, but does not reach, unity for water sticking on water ice.

ACKNOWLEDGMENTS

[1] K. Christmann, *Introduction to Surface Physical Chemistry* (Springer-Verlag, New York, 1991).

[2] S. Solomon, Nature **347**, 347 (1990).

[3] R. P. Turco, O. B. Toon, and P. Hamill, J. Geophys. Res. – Atmos. **94**, 16493 (1989).

[4] D. A. Estrin, J. Kohanoff, D. H. Laria, and R. O. Weht, Chem. Phys. Lett. **280**, 280 (1997).

[5] A. Al-Halabi, A. W. Kleyn, and G. J. Kroes, J. Chem. Phys. **115**, 482 (2001).

[6] M. J. Isakson and G. O. Sitz, J. Phys. Chem. A **103**, 2044 (1999).

[7] D. R. Haynes, N. J. Tro, and S. M. George, J. Phys. Chem. **96**, 8502 (1992).

[8] B. Lindblad, Nature **135**, 133 (1935).

[9] L. Hornekaer, A. Baurichter, V. V. Petrunin, D. Field, and A. C. Luntz, Science **302**, 1943 (2003).

[10] C. Dijkstra, C. Dominik, S. N. Hoogzaad, A. de Koter, and M. Min, Astron. Astrophys. **401**, 599 (2003).

[11] H. J. Fraser, M. P. Collings, M. R. S. McCoustra, and D. A. Williams, Mon. Not. R. Astron. Soc. **327**, 1165 (2001).

[12] M. J. Cardillo, M. Balooch, and R. E. Stickney, Surf. Sci. **50**, 263 (1975).

[13] D. E. Brown, S. M. George, C. Huang, E. K. L. Wong, H. B. Rider, R. S. Smith, and B. D. Kay, J. Phys. Chem. **100**, 4988 (1996).

[14] E. R. Batista, P. Ayotte, A. Bilic, B. D. Kay, and H. Jonsson, Phys. Rev. Lett. **95**, 223201 (2005).

[15] H. Yuan, D. R. Killelea, S. Tepavcevic, S. I. Kelber, and S. J. Sibener, "Interfacial chemistry of poly(methyl methacrylate) arising from exposure to vacuum-ultraviolet light and atomic oxygen," J. Phys. Chem. A (in press).

[16] S. Schwegmann, H. Over, V. DeRenzi, and G. Ertl, Surf. Sci. **375**, 91 (1997).

[17] K. D. Gibson, M. Viste, and S. J. Sibener, J. Chem. Phys. **112**, 9582 (2000).

[18] G. Zimbitas, M. E. Gallagher, G. R. Darling, and A. Hodgson, J. Chem. Phys. **128** (2008).

[19] D. J. Safarik and C. B. Mullins, J. Chem. Phys. **121**, 6003 (2004).

[20] K. D. Gibson and S. J. Sibener, J. Phys. Chem. A **111**, 12398 (2007).

[21] R. S. Smith, T. Zubkov, and B. D. Kay, J. Chem. Phys. **124** (2006).

[22] J. P. Devlin, J. Chem. Phys. **112**, 5527 (2000).

[23] R. S. Smith, C. Huang, E. K. L. Wong, and B. D. Kay, Surf. Sci. **367**, L13 (1996).

[24] R. J. Speedy, P. G. Debenedetti, R. S. Smith, C. Huang, and B. D. Kay, J. Chem. Phys. **105**, 240 (1996).

[25] K. D. Gibson, N. Isa, and S. J. Sibener, J. Chem. Phys. **119**, 13083 (2003).

[26] K. D. Gibson, D. R. Killelea, and S. J. Sibener, J. Phys. Chem. C **113**, 13325 (2009).

[27] J. Harris, in *Dynamics of Gas-Surface Interactions*, edited by C. T. Rettner and M. N. R. Ashfold (The Royal Society of Chemistry, Cambridge, 1991), p. 1.

[28] M. E. Saecker and G. M. Nathanson, J. Chem. Phys. **99**, 7056 (1993).

[29] I. Benjamin, M. A. Wilson, A. Pohorille, and G. M. Nathanson, Chem. Phys. Lett. **243**, 222 (1995).

[30] S. J. Sibener and Y. T. Lee, J. Chem. Phys. **101**, 1693 (1994).

[31] A. M. Wodtke, H. Yuhui, and D. J. Auerbach, Chem. Phys. Lett. **413**, 326 (2005).